International Journal of Modern Physics B
Vol. 29 (2015) 1550111 (13 pages)

DOI: 10.1142/S0217979215501118

Design of plasmonic backcontact nanogratings for broadband and polarization-insensitive absorption enhancement in thin-film solar cell

Arezoo Firoozi* and Ahmad Mohammadi†,‡

Department of Physics, Persian Gulf University, Bushehr 75169, Iran
**arezoo.firoozi67@yahoo.com*
†*mohammadi@pgu.ac.ir*
‡*am2072@yahoo.com*

Received 22 January 2015
Revised 22 March 2015
Accepted 6 April 2015
Published 14 May 2015

We discuss the rules for designing nanostructured plasmonic backcontact of thin-film crystalline silicon solar cells using two-dimensional finite-difference time-domain (2D-FDTD) method. A novel efficient quasi-periodic plasmonic nanograting is designed. Numerical calculations demonstrate that broadband and polarization-insensitive absorption enhancement is achieved by the proposed structure which is based on a supercell geometry containing N subcells in each of which there is one Ag nanowire deposited on the backcontact of the solar cell. The proposed structure offers the possibility of controlling the number and location of photonic and plasmonic modes and outperforms the periodic plasmonic nanogratings which only utilize plasmonic resonances. We start by tuning the plasmonic mode of one subcell and then construct the supercell based on the final design of the subcell. Our findings show that with a proper choice of key parameters of the nanograting, several photonic and plasmonic modes can be excited across the entire spectral region where crystalline silicon (c-Si) is absorbing. The absorption enhancement is significant, particularly in the long wavelength region where c-Si is weakly absorbing.

Keywords: Thin-film solar cells; surface plasmon polariton; waveguide mode; nanograting; FDTD method.

PACS numbers: 88.40.H-, 88.40.hj, 78.67.Qa, 02.70.-c

1. Introduction

Thin-film solar cells have attracted a great deal of attention due to their potential to reduce the cost of energy consumption. However, the efficiency of thin-film solar cells is limited because of weak absorption of the incident light in the thin absorbing

‡Corresponding author.

layer. Hence, various light trapping techniques have been proposed to enhance the efficiency of thin-film solar cells, such as antireflection coatings (AR),[1,2] reflective substrate and textured surface,[3,4] photonic crystals,[5,6] metallic nanoparticles,[7–9] periodic metallic nanogratings[10–12] and dielectric gratings.[13–15]

An interesting technique for enhancing light absorption in thin-film solar cells involves the use of metallic nanostructures to excite surface plasmon polaritons (SPPs). SPPs are electromagnetic excitations propagating at the interface between a dielectric and a metal, evanescently confined in the perpendicular direction.[16] Upon excitation, SPPs generate a strong near-field in the proximity of the nanostructures. Since optical absorption in solar cells is proportional to the electric field squared, the strong near-field causes a large optical absorption. A common way to excite SPP in solar cells is to utilize periodic plasmonic nanostructures at the bottom of absorbing layer.[17–23] It is shown that by properly optimizing backcontact nanogratings, considerable absorption enhancement is achieved.[24] However, the periodic structure can excite only one strong SPP resonance in the long wavelength range in transverse magnetic (TM) mode (the electric field component is in the plane), and has no considerable benefit for transverse electric (TE) mode (the magnetic field component is in the plane).[17]

In this work, we design a crystalline silicon solar cell with quasi-periodic plasmonic backcontact which is capable of exciting several photonic and plasmonic modes over a broad spectral range leading to a broadband absorption enhancement for both TE and TM modes. While periodic plasmonic backcontact can only excite SPP mode in the long wavelength region and quasi-periodic structures are utilized for the excitation of photonic modes,[25,26] our design is capable of controlling both plasmonic and photonic modes in the wavelength region of interest. Although, for demonstrative purposes, very thin crystalline silicon (c-Si) layer is considered as the absorbing material, the presented designing rules can be easily adopted for various semiconductors and thicknesses. The advantages of our design are as follows: (1) Fabrication of such structure is technologically feasible, (2) it can excite both planar waveguides and plasmonic modes in the long wavelength range where c-Si has a very weak absorption, (3) the number and location of modes can be adjusted through a broad parameter space. We begin by periodic plasmonic nanogratings to tune the shape and location of SPP resonances in the wavelength range of our interest. To this end, the role of key parameters such as period, height and width of nanogratings is discussed. Then, the final design is used as the base element for generating the supercell. We then discuss the effect of supercell key parameters on the number of photonic modes. To investigate the underlying physics of light trapping by the proposed structure, diffraction by nanogratings is examined. Two-dimensional finite-difference time domain (2D-FDTD) method is employed to perform all required calculations, including light absorption spectra, near-field distribution in the absorbing layer, diffraction, Fabry–Perot (FP), planar waveguide and plasmonic modes.

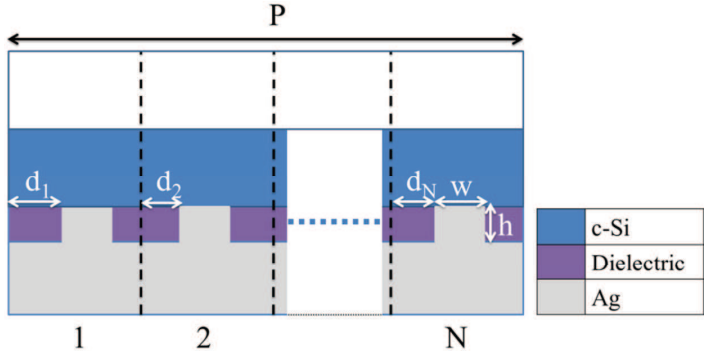

Fig. 1. (Color online) Schematic of the quasi-periodic nanograting deposited on the back side of the solar cell. The supercell period (P), width (w), height (h) and location ($d_1, d_2, \ldots, d_N$) of nanowires are indicated.

2. Structure Design and Simulation Details

To provide simple guidelines for the design of an optimum structure, we consider a simple geometry as an illustrative model. The attained design rules can be easily adopted for more realistic models of solar cells. The proposed structure consisting of an active layer and a nanostructured plasmonic backcontact is illustrated in Fig. 1. The Ag layer at the bottom of absorbing layer acts as a backcontact and as a substrate for Ag nanogratings. The quasi-periodic nanogratings are composed of N subcells in each of which there is one Ag nanowire. The grating gaps are filled with a dielectric material with the refractive index of n. This design can efficiently excite numerous photonic and plasmonic modes and provide multiple parameters for optimization through tuning the shape and location of optical resonances within the wavelength range of interest. The whole structure is characterized by a period (P), height (h) and width (w) of nanowires, and d_i ($i = 1, 2, \ldots, N$) indicating the position of each nanowire in the related subcell. Therefore, considering either $N = 1$ or $d_1 = d_2 = \cdots = d_N$ identifies the periodic nanogratings.

To evaluate the performance of the structures under investigation in the excitation of optical modes and calculate absorption spectra, we employ 2D-FDTD method.[27] The FDTD method is a versatile computational technique which directly solves the time-dependent Maxwell's equations using second-order accurate central difference in time and space and takes into account both electric and magnetic fields. The FDTD method has been significantly improved to be used in various applications in nanooptics and nanophotonics.[28–30]

We utilize the FDTD method for all kinds of calculation required for this study, including calculation of absorption, FP and SPP resonances, planar waveguide modes and diffraction. The simulation spaces are illustrated in Fig. 2. The top and bottom sides of the computational domains are terminated with perfectly matched layers (PMLs).[27] Periodic boundary conditions (PBC)[27] are employed along the left- and right-hand sides due to the periodic nature of the structures. To implement

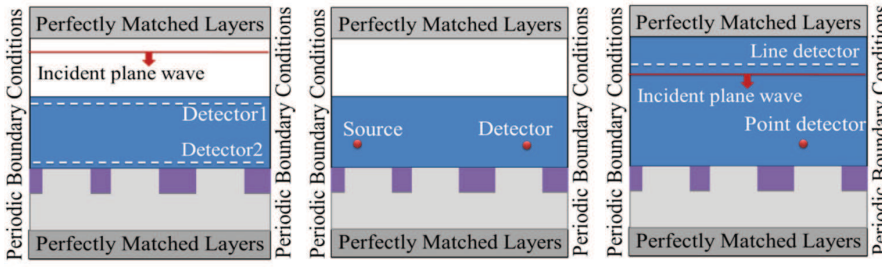

Fig. 2. (Color online) Schematic of the FDTD simulation geometries to calculate: (a) Absorption in the c-Si layer, (b) waveguide modes and (c) diffraction and SPP modes, where a line detector is used to calculate near- to far-field transformation and a point detector is used for SPP mode calculation.

the dispersive media in the FDTD method, we use Drude–Lorentz dispersion model for Ag, fitted to optical data from Johnson and Christy[31] and the optical constant of Si has been treated within the FDTD using a Lorentz dispersion model, fitted to optical data from Palik.[32] For calculating absorption spectra, diffraction and SPP modes, plane wave at normal incidence is injected using total field–scattered field technique (TF/SF),[27] while for waveguide mode analysis a dipole source is applied.

To calculate the absorption in the active layer, two detectors are used at the top and bottom of the absorbing layer to calculate the input $P_{\text{top}}(\lambda)$ and output $P_{\text{bottom}}(\lambda)$ power [Fig. 2(a)]. The optical absorption spectrum is computed according to $A(\lambda) = (P_{\text{top}}(\lambda) - P_{\text{bottom}}(\lambda))/P_{\text{in}}(\lambda)$, where $P_{\text{in}}(\lambda)$ is the incident power. The total absorbance integrated over the required spectral range is calculated by $\int A(\lambda)d\lambda$. The absorption enhancement is defined as the ratio of total absorption in the c-Si layer with nanostructured backcontact to the total absorption in the reference structure.

The FDTD geometry for studying planar waveguide modes in absorbing layer is depicted in Fig. 2(b). A dipole placed in the c-Si layer excites waveguide modes. By recording electromagnetic fields at the detector position and using Fourier transform, waveguide modes are calculated.

Although the grating equation gives the angles of diffracted beam, it cannot be used to estimate the fraction of energy in each diffraction order.[33] Here, we utilize the FDTD method for calculation of diffraction. The simulation space is displayed in Fig. 2(c). In this case, FP and waveguide modes cannot be excited. A line detector positioned behind the plane wave source measures the reflected light. We take advantage of a method based on near-field to far-field techniques to evaluate the reflection intensity of nanogratings.[27]

3. Results and Discussions

To obtain the guidelines for optimal design of nanostructured plasmonic backcontact for broadband absorption enhancement, we begin with periodic nanogratings

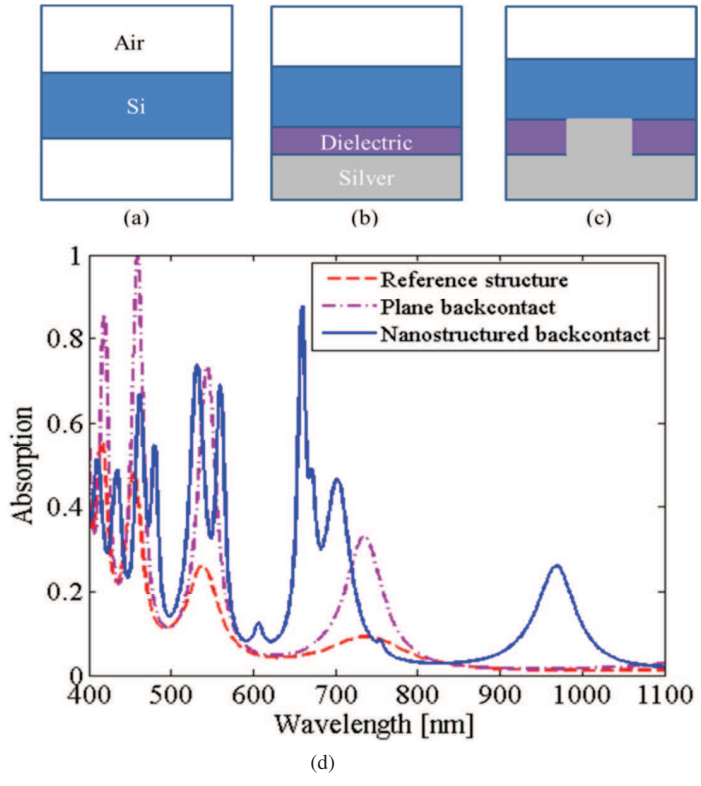

Fig. 3. (Color online) Cross-section of the simulated geometries of (a) reference structure, (b) plane backcontact, (c) nanostructured backcontact and (d) absorption in the c-Si layer for three different designs.

and investigate the impact of key parameters on the excitation of various optical modes. To this end, we calculate light absorption in the absorbing layer for three different designs: A reference structure which is a 200 nm of c-Si slab in air [Fig. 3(a)], a thin-film c-Si layer deposited on a plane backcontact consisting of 80 nm of dielectric layer with the refractive index of $n = 1.5$ and an infinitely thick back substrate of Ag [Fig. 3(b)] and a thin-film c-Si layer deposited on a nanostructured backcontact [Fig. 3(c)]. The period, height and width of nanogratings are fixed as 200, 80 and 100 nm, respectively. The incident light wavelength ranges from 400–1100 nm. The calculated absorption spectra in the active layer are shown in Fig. 3(d). For the reference structure, only FP resonances are excited in the short wavelength range. It is the same for the structure with a plane backcontact. However, in the latter case the absorption is enhanced due to stronger FP resonances. By embedding Ag nanowires within the dielectric layer, new peaks are appeared in the absorption spectrum and a small shift is observed in the FP resonances. The extra peaks in the wavelengths below 800 nm are due to the excitation of planar waveguide modes. The most important role of Ag nanograting in this case is to

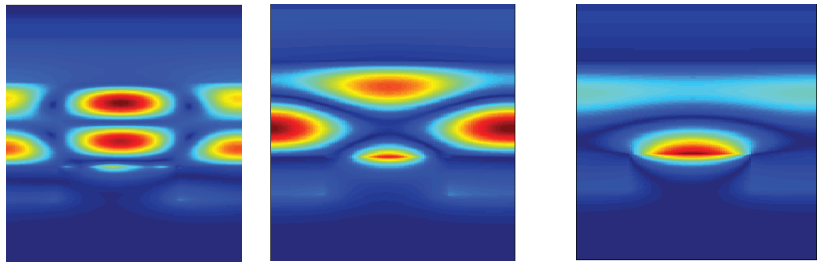

(a) (b) (c)

Fig. 4. (Color online) Magnetic field profiles inside the c-Si layer for periodic nanogratings at the bottom of absorbing layer at wavelengths of (a) 556 nm, (b) 700 nm and (c) 968 nm.

excite the SPP resonance which leads to very strong absorption enhancement in the spectral range of 800–1100 nm where c-Si has a very weak absorption. The modal calculations and the optical field profiles shown in Fig. 4 confirm the excitation of photonic and plasmonic modes.

In addition to the excitation of optical resonances, it is important to be able to tune the resonances at the wavelength range of interest. Therefore, it is necessary to investigate the effect of nanogratings parameters, including size and period of nanogratings, on the position and shape of optical resonances. To begin, we study the effect of height of nanogratings on absorption in solar cells. The thickness of the c-Si layer, width and period of nanogratings are fixed as 200, 100 and 200 nm. Light absorption in the c-Si layer as a function of wavelength with varying height of nanogratings is shown in Fig. 5(a). The plasmonic resonance shifts towards longer wavelengths when the height of nanogratings increases.

Next, we investigate the effect of width of nanogratings on the position and shape of SPP resonance. The thickness of the c-Si layer, height and period of nanogratings are fixed as: 200, 80 and 200 nm. Figure 5(b) depicts the absorption

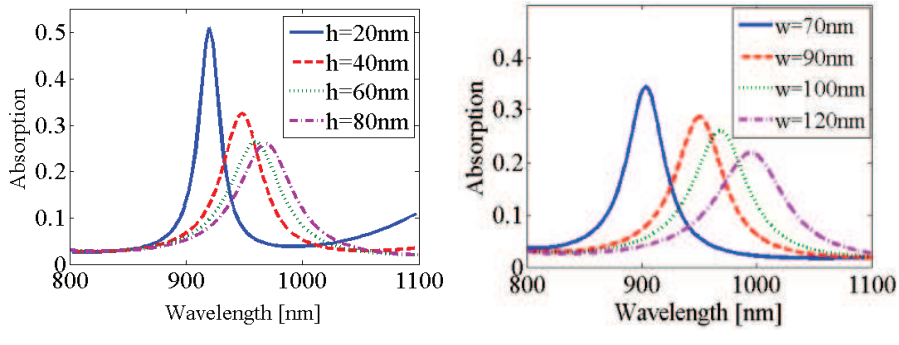

(a) (b)

Fig. 5. (Color online) Absorption in the c-Si layer with varying (a) height and (b) width of nanogratings.

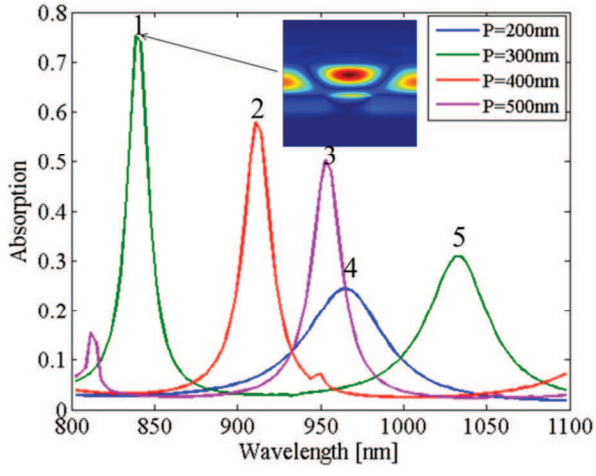

Fig. 6. (Color online) Absorption spectra of the solar cell for various periods of nanogratings. The inset shows the magnetic field profile at wavelength of 848 nm corresponding to $P = 300$ nm.

spectra for various widths of nanowire. As the width of nanograting increases, the plasmonic resonance shifts towards longer wavelengths. In all cases, although the width of plasmon resonance changes, the corresponding total absorption is almost unchanged.

Another parameter that can play an important role to shift both plasmon resonance and planar waveguide modes is the period of nanograting. To verify it, we keep constant the thickness of the absorbing layer, height and width of nanowire as 200, 80 and 100 nm and vary the period from 200 nm to 500 nm. As shown in Fig. 6, increasing period shifts SPP resonances (labeled as 4 and 5) toward longer wavelength. When the period of nanograting is 300 nm, additional enhanced absorbance feature (labeled as 1) can be observed in the long wavelength range which cannot be attributed to plasmonic modes. The magnetic field distribution at the wavelength of 848 nm, depicted in the inset of Fig. 6, confirms that it is a planar waveguide mode.

Similar to the plasmon resonance, planar waveguide modes (labeled as 1, 2 and 3) shift towards longer wavelengths by increasing the period of nanograting. It confirms that it is possible to have multiple optical modes in the wavelength range of interest which can be achieved by proper design of nanogratings. However, this goal is not reachable by just increasing the period. To verify it, we show the absorption spectra versus period in Fig. 7. The overall absorption in the wavelength range of 800-1100 nm for periods between 150 nm and 250 nm is only due to the excitation of SPP modes. As discussed, increasing period of nanograting shifts the SPP resonances toward longer wavelengths. For periods larger than 250 nm, a new peak due to the excitation of waveguide modes is appeared. By increasing the period of nanogratings beyond 300 nm, higher-order waveguide modes enter the desired

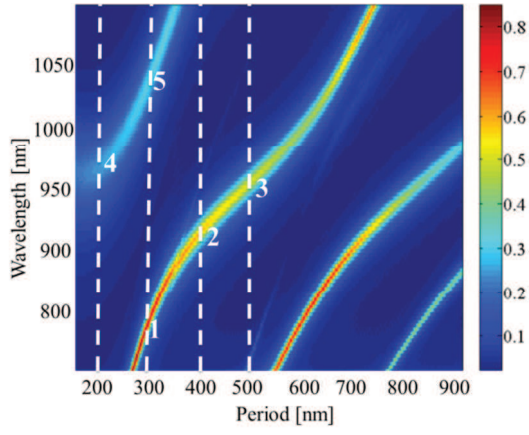

Fig. 7. (Color online) Absorption spectra versus period for the case of periodic nanogratings of 80 nm height and 100 nm width. The vertical dashed lines correspond to the absorption spectra of Fig. 6.

range and SPP resonance leaves the region. Therefore, it is not possible to keep the plasmon resonance and add more than one waveguide mode in the wavelength range of interest by increasing the period.

After designing a single periodic nanograting, we can use it as the base element to construct the quasi-periodic nanogratings including N elements ($N = 2, 3, \ldots$). It turns out that the absorption enhancement due to the SPP resonance almost remains unaffected, while more planar waveguide modes (depending on N) appear in the long wavelength region.

Figure 8(a) compares the absorption spectra calculated for quasi-periodic nanogratings with a period of 400 nm ($N = 2$), 600 nm ($N = 3$) and 800 nm

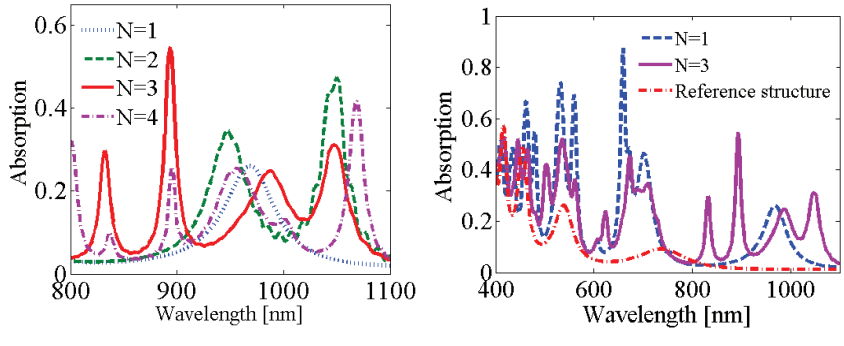

(a) (b)

Fig. 8. (a) Absorption in the c-Si layer for the periodic nanogratings ($N = 1$) and quasi-periodic nanogratings with $N = 2$, $N = 3$ and $N = 4$ in the long wavelength region and (b) comparison of light absorption in the wavelength range of 400–1100 nm for the cases of quasi-periodic ($N = 3$) with periodic ($N = 1$) nanogratings and the reference structure.

($N = 4$) with that for the periodic structure ($N = 1$) with a period of 200 nm. For $N = 1$, only one absorption enhancement peak is occurred in the long wavelength range which is due to the excitation of a surface plasmon resonance. No waveguide mode is observed in the long wavelength range. However, both plasmonic and waveguide modes are excited for N bigger than one. Therefore, the quasi-periodic nanogratings outperform the periodic ones in terms of excitation of several waveguide modes besides the SPP resonance, leading to a large absorption enhancement in the long wavelength range. Although, quasi-periodic structures with higher N can introduce more photonic modes, there is an optimal value of N for which both number of peaks in the favored wavelength region and their height are optimum. As seen in Fig. 8(a), the highest absorption enhancement for the current structure is occurred when $N = 3$, and for higher N, the absorption peaks are shifted far away from the wavelength region of interest. It is also observed in Fig. 8(b) that for the short wavelength range, adding quasi-periodic plasmonic nanogratings maintains a good absorbance comparable to the periodic nanogratings.

To understand the underlying mechanism of absorption enhancement, the magnetic field profile inside the absorbing layer corresponding to the resonance wavelengths of 832, 893.5, 988 and 1047 nm are depicted in Figs. 9(a)–9(d). The figures confirm the excitation of photonic and plasmonic modes, and coupling between these modes due to employing quasi-periodic nanogratings at the bottom of the absorbing layer. The strong field at the Ag/c-Si interfaces demonstrates the excitation

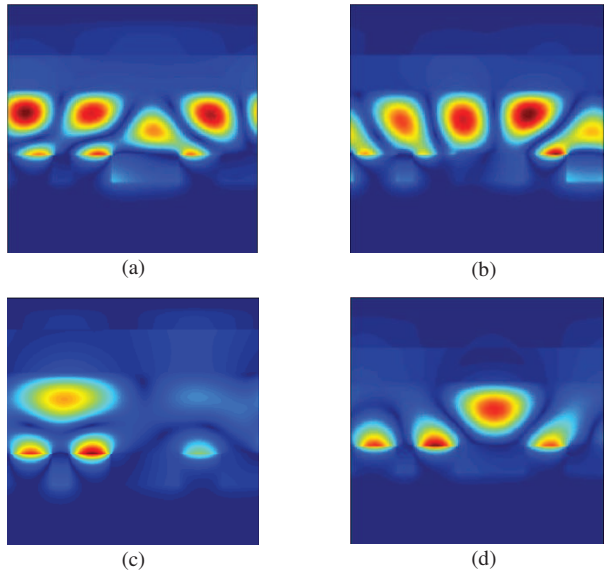

Fig. 9. (Color online) Magnetic field profiles inside the c-Si layer for the quasi-periodic nanogratings at the bottom of absorbing layer at the wavelengths of (a) 832 nm, (b) 893.5 nm, (c) 988 nm and (d) 1047 nm.

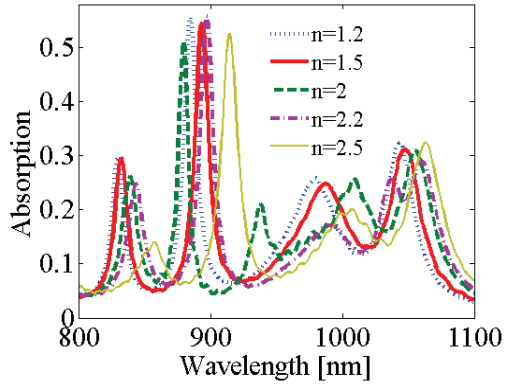

Fig. 10. (Color online) The effect of refractive index of dielectric material on the absorption enhancement.

of plasmonic modes, and the strong field confinement inside the c-Si layer reveals the excitation of photonic modes. Coupling between plasmonic and photonic modes is observed in the figures.

Next, we investigate the effect of the additional degree of freedom, the refractive index of the embedding material, on the light absorption in the absorbing layer. In Fig. 10, absorption in the active layer in the wavelength range of 800–1100 nm for the quasi-periodic nanogratings ($N = 3$) embedded in different dielectric materials are plotted. The refractive index of embedding material is varied from 1.2 to 2.5. In the case of $n = 2$, additional absorption enhancement peak at the wavelength of 938 nm can be observed which is due to the excitation of a planar waveguide mode. Despite of that, the total absorption for $n = 1.5$ is higher. Therefore, we will consider $n = 1.5$ for the next calculations. It should be noted that the optimum value for n depends on the absorbing material and the subcell parameters.

To better understand the differences between periodic and quasi-periodic structures in exciting waveguide modes in the long wavelength range, we compare the back-diffracted light by nanogratings. The FDTD calculation space is depicted in Fig. 2(c). For both cases we consider a period of 600 nm with equal and nonequal distances between nanowires for periodic and quasi-periodic structures, respectively. As shown in Fig. 11, the quasi-periodic nanogratings can diffract back the incident light with angles higher than critical angles into the absorbing layer, leading to coupling of incident light to waveguide modes. The periodic structure reflects back the light mainly in the zeroth-order of diffraction. It is known that larger period can couple light into more diffraction orders and may excite a larger number of photonic resonances. However, these resonances are rather weak, since small fraction of incident light is coupled into each mode. Moreover, considerable fraction of incident light is diffracted into angles smaller than the critical angle, and is passed through the absorbing layer without total internal reflection. Therefore, it is necessary to find the optimal value for the period and the distances between nanowires in order

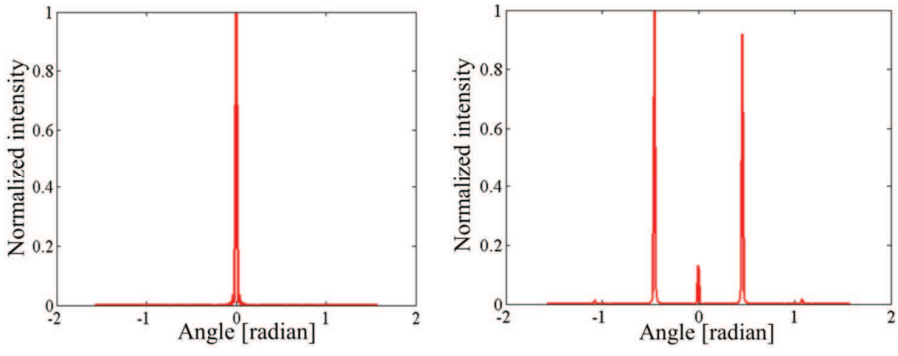

(a) (b)

Fig. 11. Normalized reflected intensity distribution of (a) periodic and (b) quasi-periodic nanogratings with a period of 600 nm corresponding to wavelength of 962 nm.

to excite a few diffraction orders with enough energy. The proposed design offers the possibility to control the direction and the amplitude of light diffracted in each order.

As discussed, quasi-periodic structure can excite planar waveguide modes in addition to SPP resonances in the wavelength range of our interest. This issue becomes more important when the illumination is TE-polarized which cannot excite SPP resonances. In this case, the periodic plasmonic nanograting either has negative or very small effect on enhancing optical absorption. To show the effectiveness of the proposed structure for TE mode, we calculate the absorption spectrum for a quasi-periodic structure with the period of 600 nm which consists of three subcells ($N = 3$). The gap between plasmonic nanogratings is filled with a dielectric material with the refractive index of 1.5. The calculated absorption spectrum compared to the case of periodic structure ($N = 1$) with $P = 200$ nm and the reference structure is depicted in Fig. 12. It is observed that quasi-periodic nanogratings can excite photonic modes in the long wavelength leading to a broadband absorption enhancement.

Finally, we investigate the performance of our final design ($N = 3, n = 1.5$) across the entire spectral region for both TM and TE polarizations. Light absorption in the active layer as a function of wavelength compared to the reference structure is depicted in Fig. 13. It is observed that a broadband and polarization-insensitive absorption enhancement over a broad wavelength range of 400–1100 nm is achieved due to the excitation of several photonic and plasmonic modes. As it is evident, the quasi-periodic nanogratings outperform the periodic counterpart for both TM and TE cases. The absorption enhancement of supercell, as compared to that of the periodic structure, is about 7% for TM polarization and about 21% for TE polarization. It is remarkable since the only difference between two cases is the position of nanowires in the subcells. Therefore, considerable enhancement is achieved by properly designing the nanostructured backcontact. It should be noted

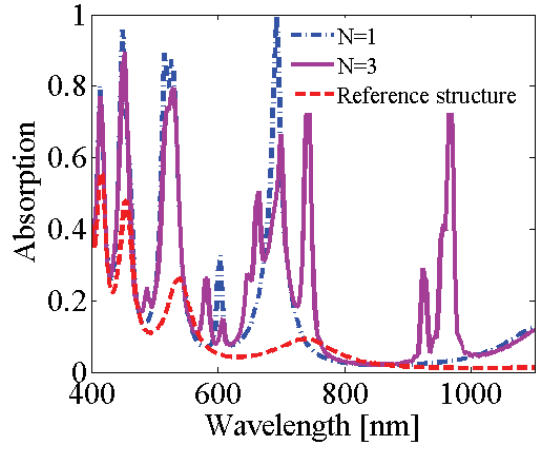

Fig. 12. (Color online) Absorption in the c-Si layer for the quasi-periodic nanogratings ($N = 3$), periodic nanogratings ($N = 1$) and reference structure under TE-polarized plane wave.

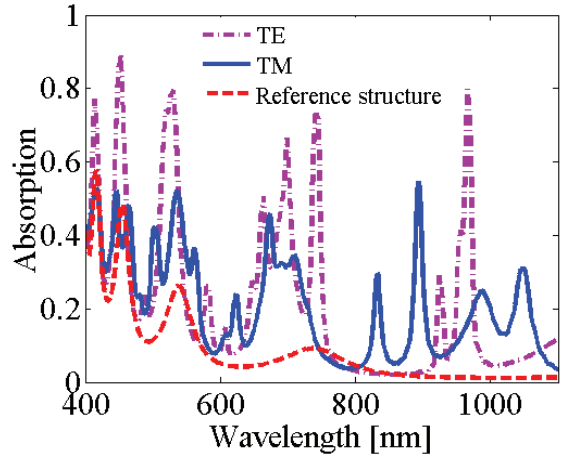

Fig. 13. (Color online) Absorption in the active layer for TE and TM polarizations.

that the structure under investigation is not fully optimized; hence, even further enhancement can be achieved by optimizing all degrees of freedom.

4. Conclusion

Quasi-periodic plasmonic backcontact solar cells were proposed and designed for effective light trapping to enhance optical absorption in c-Si layer. We have shown that by choosing the proper value of key parameters, including period, height and width of nanowires and the refractive index of embedding dielectric material, the number and locations of photonic and plasmonic modes can be adjusted across the

wavelength range of our interest. In comparison to the periodic structure, quasi-periodic nanogratings can excite several photonic and plasmonic modes across the entire spectral region, particularly in the long wavelength region where c-Si is weakly absorbing. Therefore, a significant broadband and polarization-insensitive absorption enhancement is achieved for both TM and TE cases.

Acknowledgments

The authors are thankful to Dr. Aimi Abass for helpful discussions. This work was supported by the Persian Gulf University Research Council.

References

1. J. N. Munday and H. A. Atwater, *Nano Lett.* **11**, 2195 (2011).
2. Y. J. Lee *et al.*, *Nano Lett.* **8**, 1501 (2008).
3. E. Yablonovitch and G. D. Cody, *IEEE Trans. Electron Devices* **29**, 300 (1982).
4. J. Zahao *et al.*, *Appl. Phys. Lett.* **73**, 1991 (1993).
5. G. Gomard *et al.*, *J. Appl. Phys.* **108**, 123102 (2010).
6. Y. Park *et al.*, *Opt. Express* **17**, 14312 (2009).
7. A. P. Kulkarni *et al.*, *Nano Lett.* **10**, 1501 (2010).
8. H. A. Atwater and A. Polman, *Nature Mater.* **9**, 205 (2010).
9. V. E. Ferry, J. N. Munday and H. A. Atwater, *Adv. Mater.* **22**, 4794 (2010).
10. S. Xiao, E. Stassen and N. A. Mortensen, *J. Nanophotonics* **6**, 061503 (2012).
11. B. Z. Li *et al.*, *J. Mod. Opt.* **58**, 796 (2011).
12. V. E. Ferry *et al.*, *Opt. Express* **18**, A237 (2010).
13. S. Das *et al.*, *J. Mod. Opt.* **60**, 556 (2013).
14. S. Das *et al.*, *J. Mod. Opt.* **59**, 1219 (2012).
15. M. B. Duhring, N. A. Mortensen and O. Sigmund, *Appl. Phys. Lett.* **100**, 211914 (2012).
16. S. A. Maier, *Plasmonics: Fundamentals and Applications* (Springer, New York, 2007).
17. R. B. Dunbar, T. Pfadler and L. S. Mende, *Opt. Express* **20**, A177 (2012).
18. E. Battal *et al.*, *Opt. Express* **20**, 9458 (2012).
19. A. Abass *et al.*, *J. Appl. Phys.* **109**, 023111 (2011).
20. M. A. Sefunc, A. K. Okyay and H. V. Demir, *Opt. Express* **19**, 14200 (2011).
21. X. Tian *et al.*, *J. Mod. Optics* **61**, 1 (2014).
22. I. Kim *et al.*, *Opt. Express* **20**, A729 (2012).
23. W. Wang *et al.*, *Nano Lett.* **10**, 2012 (2010).
24. L. Shi, Z. Zhou and B. Tang, *Optik* **125**, 789 (2014).
25. E. R. Martins *et al.*, *Phys. Rev. B* **86**, 041404 (2012).
26. E. R. Martins *et al.*, *Nat. Commun.* **4**, 2665 (2013).
27. A. Taflove and S. Hagness, *Computational Electrodynamics: The Finite-Difference Time-Domain Method* (Artech House, Norwood, 2005).
28. A. Mohammadi, H. Nadgaran and M. Agio, *Opt. Express* **13**, 10367 (2005).
29. T. Jalali *et al.*, *J. Comput. Theor. Nanosci.* **4**, 644 (2007).
30. A. Mohammadi, V. Sandoghdar and M. Agio, *New J. Phys.* **10**, 105015 (2008).
31. P. B. Johnson and R. W. Christy, *Phys. Rev. B* **6**, 4370 (1972).
32. E. D. Palik and G. Ghosh (eds.), *Handbook of Optical Constants of Solids* (Academic Press, San Diego, 1998).
33. B. E. A. Saleh and M. C. Teich, *Fundamentals of Photonics* (John Wiley, 1991).